Int. J. Heat Mass Transfer. Vol. 29, No. 8, pp. 1169–1176, 1986
Printed in Great Britain

0017–9310/86 $3.00 + 0.00
Pergamon Journals Ltd.

Aging of polyurethane foams

A. G. OSTROGORSKY,* L. R. GLICKSMAN* and D. W. REITZ†

*M.I.T. Department of Mechanical Engineering, Cambridge, MA 02139, U.S.A.
† Owens Corning Fiberglass Corporation, Granville, OH 43221, U.S.A.

Abstract—The degradation of foam thermal properties due to the diffusion of the air into the foam, termed the foam aging, is a major drawback of polyurethane foams. An analytical model was developed to predict the effective diffusion coefficient of the foam and from it the rate of gas diffusion and foam aging. The model requires a measurement of the wall permeability and foam internal geometry. An experimental steady-state technique was developed to measure the permeability of the cell walls. To check the models an experimental technique was developed to measure the foam effective diffusion coefficient. The model predictions of the effective diffusion coefficient were found to be within 29% of the foam data or better.

1. INTRODUCTION

HEAT is transferred through closed-cell foam insulation by conduction through the solid polymer making up the cell structure, by conduction through the gas within the cells and by thermal radiation; because of the small cell size there is no convective heat transfer. At least 50% of the heat is transferred by conduction through the gas so that it is advantageous to have a low conductivity gas inside of the foam, for example fluorocarbon 11 (R-11). The total conductivity of the polyurethane foam is only two-thirds of the conductivity of stagnant air, while open-cell foam and glassfiber insulation have 1.3–2 times the conductivity of stagnant air.

The increase of foam conductivity with age, i.e. the aging effect, is a major drawback of the closed-cell foams. Aging occurs as air components diffuse into the foam while R-11 vapor diffuses out. Air components diffuse much faster than freon so that the aging process can be divided into two stages: the diffusion of the air components, which lasts typically 1 year for a 2.5-cm (1-in)-thick sample, and diffusion of R-11, which is expected to last approximately 20 times longer. At present, few data have been published on the diffusion coefficients of the slowest diffusing gases, N_2 and R-11. Most of the published data were obtained from indirect [1, 2], or transient measurements [3, 4]. Data obtained by different investigators vary by more than one order of magnitude [5].

Once the effective diffusion coefficients of R-11 and air components are determined, they can be used in the transient diffusion equation to predict the change of the gas composition with time in foams. The effective foam diffusion coefficient can be determined by lengthy foam-permeability measurements (which give little physical insight into foam aging behavior) or can be evaluated based on the knowledge of the foam geometry and permeability of the solid polymer cell walls. The important geometry parameters are: cell wall thickness, cell size, arrangement, elongation and percent of open cells.

Analytical models of the effective diffusion coefficient have been developed in the past [2, 6]. However, they assumed oversimplified geometries with unrealistically thick cell walls. In addition they could not be validated because the published data of foam diffusion coefficient varied substantially.

The existing data on the cell wall permeability coefficient are also uncertain. Some data on solid polyurethane have been published [7], but it is not known if the foam cell walls have the same permeability coefficient since they have different formation and thermal history. Reitz [8] measured the permeability of the cell walls obtained from large bubbles that are often created on the free rise foam surface; he obtained data on cell wall permeability to O_2 and CO_2.

Reitz suggested a model with an accurate distribution of solid polymer [9]. He determined that cell walls contain only 10–20% of the total polymer material. He also developed an embedding technique to obtain a clear two-dimensional view of the foam structure.

The embedding technique described in refs. [8, 9] will be briefly summarized. A new model relating the effective foam diffusion coefficient to cell wall permeability, cell wall thickness and average distance between the cell walls along with the experimental techniques for measurement of foam and cell wall permeability coefficients are presented in this paper.

2. FOAM GEOMETRY MEASUREMENT

To analyze quantitatively foam cellular geometry, the exposed cell layers at the surface of a foam sample were filled with a resin which solidified without altering the foam structure. After curing, the resin and foam composite can be cut into thin sections to obtain a flat, cross-sectional view of the foam's cell structure. A typical section of polyurethane in Fig. 1 shows the resin within the cells surrounded by the polymer which forms an interconnecting

NOMENCLATURE

A	area [cm^2]	T	temperature [°C]
C	concentration [cm$^3_{STP}$ cm^{-3}]	t	thickness [cm].
d	cell diameter [cm]		
D	diffusion coefficient [cm^2 s^{-1}]		
J_m	mass flux [cm$^3_{STP}$ cm^{-2} s^{-1}]	Greek symbols	
E	activation energy [J]	ε	enhancement parameter.
$\langle l \rangle$	average distance between successive membranes [cm]		
L	length [cm]	Subscripts	
n	number of intersections	c.w.	cell wall
p	gas pressure [atm]	eff	effective
Pe	permeability [cm$^3_{STP}$ cm^{-1} s^{-1} atm^{-1}]	p	polyurethane
Pe_0	reference value of Pe	SM	successive membrane
R	resistance [atm s cm$^{-3}_{STP}$]	STP	standard temperature and pressure
S	solubility coefficient [cm$^3_{STP}$ cm^{-3} atm^{-1}]	x-s	cross-section

cellular structure. Observations of a foam's cell structure in an optical microscope reveal that it is comprised of two basic structural elements. Thin polymeric membranes form the walls of the cells. At the intersection of three cell walls, a build-up of polymer material forms rod-shaped members termed struts. Since only the cell walls resist diffusion, it is of primary interest to determine the average distance between the cell walls and their thickness. The average distance between the cell walls is measured by drawing random lines across the photograph of embedded foam sections and counting the number of intersections with the cell walls

$$\langle l \rangle = L/n \tag{1}$$

where n is the total number of intersections and L is the total length of the lines. If cells are elongated, the lines should be drawn parallel to the flow direction. The thickness of the cell walls can be measured from scanning electron microscope photographs of unembedded foam.

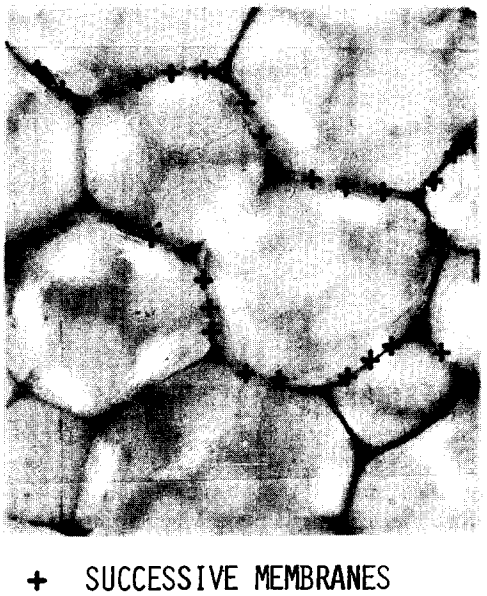

FIG. 1. Two-dimensional view of cell structure using embedding resin showing cell walls grouped into successive membranes.

3. PERMEATION THROUGH POLYMERIC MEMBRANES

When a polymeric membrane such as a wall of a closed-cell foam is exposed to a gas, gas molecules are absorbed and desorbed at the membrane surface. The mass flow rate of one gas species as it diffuses across the membrane is

$$J_m = Pe/t(p_2 - p_1) \tag{2}$$

where p_1 and p_2 are the low and high partial pressure imposed on the two surfaces, respectively; Pe is the permeability coefficient of the gas species through solid polymer; and t is the membrane thickness. The partial pressure of that gas species directly above the surface can be related to the concentration inside of the membrane next to the surface by Henry's Law

$$C = Sp \tag{3}$$

where S is the solubility coefficient which can be assumed independent of pressure level.

Combining Henry's Law with equation (2), one gets

$$J_m = (Pe/S)/t(C_2 - C_1). \tag{4}$$

The diffusion coefficient of a gas through the membrane is defined as

$$J_m = D/t(C_2 - C_1). \tag{5}$$

Thus

$$Pe = DS. \quad (6)$$

Although molecules of the air components N_2, O_2 and CO_2 have roughly the same molecular size, the results will show that their permeation rates through a membrane vary substantially. The diffusion coefficient of the three gases is approximately equal [10]. Therefore according to equation (5) their diffusion rate under the same concentration gradient is also approximately equal. However, the air components have different solubilities [10] and therefore they have different concentration gradients, according to equation (3). Consequently their permeation rate is quite different, equation (2), even when the pressure difference of the gas adjacent to the membrane surfaces is the same.

It is customary to use units cm^3_{STP} for the amount of gas in cm^3 at standard temperature, (298 K) and standard pressure (1 atm) [10]. Then, units of the mass transport properties are: D, $cm^{-2}\ s^{-1}$; Pe, $cm^3_{STP}\ cm^{-1}\ s^{-1}\ atm^{-1}$; and S, $cm^3_{STP}\ cm^{-3}\ atm^{-1}$, while the mass flux has units $cm^3_{STP}\ cm^{-2}\ s^{-1}$.

4. THE MODEL OF GAS STORAGE CAPACITY IN CLOSED-CELL FOAMS

In closed-cell foams the solid polymer and the voids store gases. According to Norton [2], the solubility of the solid polymer to air components is less than 0.1 $cm^3_{STP}\ cm^{-3}\ atm^{-1}$. By definition, 1 cm^3 of a void space at standard temperature and pressure contains 1 cm^3_{STP} of gas. For 35.2 kg m^{-3} (2.2 lb ft^{-3}) foam, the solid polymer is 2.4% of the foam volume while pore space occupies 97.6%. This implies that the solid stores less than 1% of the gas. For practical applications, the solubility of the solid can be neglected. Consequently, the mass storage capacity of the foam (or the effective foam solubility) can be modeled as the storage capacity of the voids.

The ideal gas law can be used to determine the amount of matter than can be stored per unit of volume and unit of pressure in the voids. The concentration of an ideal gas in voids is

$$C = p/(RT). \quad (7)$$

At standard temperature and pressure, concentration is equal to

$$C_{STP} = p_{STP}/(T_{STP}R). \quad (8)$$

By combining equations (7) and (8) we obtain

$$C = C_{STP}(p/p_{STP})(T_{STP}/T). \quad (9)$$

Neglecting the concentration of gases in the solid polymer, from equation (9), the effective concentration of a gas in a closed-cell foam is

$$C_{eff} = C_{STP}(p/p_{STP})(T_{STP}/T). \quad (10)$$

We can define an effective foam solubility by dividing equation (11) by p

$$S_{eff} = C_{eff}/p = C_{STP}/p_{STP}(T_{STP}/T) = S_{eff,STP}(T_{STP}/T). \quad (11)$$

Note that $S_{eff,STP}$ is equal to 1 $cm^3_{STP}\ cm^{-3}\ atm^{-1}$ for all the gases. Then equation (11) takes the simple form,

$$S_{eff} = T_{STP}/T\ cm^3_{STP}\ cm^{-3} atm^{-1}. \quad (12)$$

Equation (11) or (12) model the effective foam solubility (i.e. the foam storage capacity) with high accuracy as long as the gas follows the ideal gas law; no measurement is needed. It is important to note that foam mass storate capacity decreases linearly with $1/T$.

Some types of fluorocarbons can condense inside the closed cells. Equation (11) can not be used if any substantial condensation of the transported gas occurs.

5. THE SUCCESSIVE MEMBRANES MODEL FOR PERMEABILITY AND DIFFUSION COEFFICIENTS IN FOAMS

The measured polymer permeability can be combined with the measured foam-geometry parameters to obtain an overall model of gas diffusion in foam insulation. For a typical foam application the thickness of a foam slab is much larger than the average cell diameter, so that a continuum model for the foam can be employed. The model includes the following assumptions:

- Each cell wall membrane is considered a resistance to gas permeation. The permeation resistance inside the cells is neglected.
- No pores exist in the cell walls.
- The gas flow lines are parallel to the partial pressure gradient.

Consider a volume of foam having cross-sectional area $A_{x\text{-}s}$ perpendicular to the partial pressure gradient and having length L. For cells of equal wall thickness the resistance of successive membranes can be summed to give the effective foam resistance to permeation

$$R_{foam} = nR_{c.w.}. \quad (13)$$

The cell walls can be modeled as successive membranes (SM), Fig. 1. The resistance of a single non-plane successive membrane is defined as

$$R_{c.w.} = t/(A_{SM}Pe_{c.w.}) \quad (14)$$

where A_{SM} is the membrane area with the cross-section $A_{x\text{-}s}$. If the membrane area is planar, parallel to $A_{x\text{-}s}$, then A_{SM} equals $A_{x\text{-}s}$. Otherwise the membrane area will be larger than $A_{x\text{-}s}$.

Combined equations (13) and (14) yield

$$R_{foam} = nt/(A_{SM}Pe_{c.w.}). \quad (15)$$

We can redefine the foam resistance to permeation in terms of the foam effective permeability

$$R_{\text{foam}} = L/(A_{\text{x-s}} Pe_{\text{eff}}). \tag{16}$$

By equating (15) and (16) we get

$$Pe_{\text{eff}} = (A_{\text{SM}}/A_{\text{x-s}})L/(nt)Pe_{\text{c.w.}} \tag{17}$$

or by using (1)

$$Pe_{\text{eff}} = (A_{\text{SM}}/A_{\text{x-s}})\langle l\rangle/t\, Pe_{\text{c.w.}}. \tag{18}$$

We can define

$$\varepsilon = A_{\text{SM}}/A_{\text{x-s}}. \tag{19}$$

Then, the equation (18) can be rewritten as

$$Pe_{\text{eff}} = \varepsilon\langle l\rangle/t\, Pe_{\text{c.w.}} \tag{20}$$

Equation (19) defines an important geometric parameter: the ratio of the membrane area to the flow cross section. We will refer to parameter ε as the enhancement parameter. This parameter accounts for the fact that the cell walls are curved. The curved cell walls form nonplanar membranes whose area is larger than the area of the membrane project normally to the flow direction. According to equation (14) a larger membrane area results in less permeation resistance and the foam effective permeability coefficient increases.

Assuming spherical cell structure we can obtain $\varepsilon = 2$, by dividing the area of one-half of a sphere with its projected area.

An alternative approach to compute ε assumes that cell walls forming successive membranes are randomly oriented planes. The ratio of area of randomly oriented planes and their projected area can be readily shown to be equal to 2.

The effective foam permeability coefficient can be now modified to account for the enhancement

$$Pe_{\text{eff}} = 2\langle l\rangle/t\, Pe_{\text{c.w.}}. \tag{21}$$

The definition (6) can be rewritten in this form:

$$D_{\text{eff}} = Pe_{\text{eff}}/S_{\text{eff}}. \tag{22}$$

By combining equations (21), (11) and (22) we finally obtain the model for the effective diffusion coefficient:

$$D_{\text{eff}} = 2\langle l\rangle/t\, Pe_{\text{c.w.}}(T/T_{\text{STP}})/S_{\text{eff,STP}}. \tag{23}$$

$S_{\text{eff,STP}}$ is equal to 1 $\text{cm}^3_{\text{STP}}\,\text{cm}^{-3}\,\text{atm}^{-1}$ for all the gases. From equation (23), if cm^3_{STP} is used as unit of mass, at standard temperature and pressure, D_{eff} and Pe have the same numerical value but different units. Then

$$D_{\text{eff}} = 2\langle l\rangle/t\, Pe_{\text{c.w.}}(T/T_{\text{STP}})\ \text{cm}^{-2}\,\text{s}^{-1}. \tag{24}$$

Note that $Pe_{\text{c.w.}}$ is exponentially temperature dependent, and follows an equation of Arrhenius type

$$Pe_{\text{c.w}} = Pe_0 \exp\left[-E/(RT)\right] \tag{25}$$

where E is the activation energy of permeation, and Pe_0 is the exponential constant.

6 MEASUREMENT OF THE CELL WALL POLYMER PERMEABILITY COEFFICIENT

The permeability of the membrane can be related to the measured flow as given by equation (2). To obtain cell walls for permeability measurements, samples were taken from large bubble-cells which are created on the surface of free-rise foam. These bubbles have the same composition and a thickness which is the same order of magnitude as the walls of the normal size cell. They also have approximately the same thermal history as other cell walls, a factor that might have an influence on the polymer permeability.

To measure the permeability of the membranes, a volumetric type apparatus was designed and built (Fig. 2). Since the membranes are very thin and fragile they are exposed to a concentration difference rather than a substantial total pressure difference. One side of the membrane is exposed to the test gas at atmospheric pressure while the other side is exposed to freon gas at atmospheric pressure. Freon permeates much slower than any air component, so that its permeation can be neglected during tests of other gases. The test membrane is small, about 7 mm in diameter, resulting in a very low volumetric flow of air through the membrane. Due to the low flow, any outgassing from other materials in the apparatus or temperature variation could seriously disturb the measurement. For that reason the whole cell was made from materials used in high vacuum applications. The membranes were fixed to a stainless-steel mounting ring by Sealstic cement, while the cell was sealed by indium gaskets. A capillary tube having a 0.5 ± 0.005 mm diameter was also sealed to the cell to allow the measurement of the volume of the permeated gas. The volume was measured by measuring the change of the position of a methyl isolbutyl ketone slug placed in the tube. The recent data for the lower permeability gases, were taken with an absolute pressure transducer

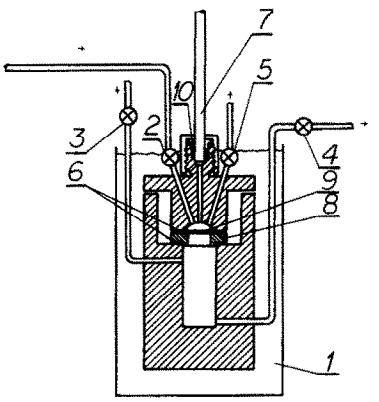

FIG. 2. Volumetric-type apparatus for cell wall permeability measurement. 1, constant temperature bath; 2 and 3, metering valves; 4 and 5, valves; 6, indium gaskets; 7, capillary tube; 8, membrane; 9, mounting ring; 10, indium O-ring.

so that change of pressure, rather than change of volume, was measured. This change was made because at low permeation rates the capillary techniques introduces two errors. The liquid slug in the capillary vaporizes slightly and creates additional slug motion. Changes in barometric pressure also influence the capillary measurement. The cell was placed in an ethyl alcohol constant-temperature bath which was kept within $\pm 0.03°C$. The temperature of the test gas and the freon was measured continuously while the room temperature was also maintained within $\pm 0.5°C$ since it was noticed that a temperature change of the valves partially outside the alcohol also disturbed the measurement. All parts of the cell in contact with gas were cleaned ultrasonically. Both the cell and membrane samples were kept in a vacuum when data were not taken.

Special care has to be devoted to membrane selection. Membranes having micro-cracks or bubbles should not be used. Defects are much more likely to occur in the walls of these comparatively large membranes than in the much smaller membranes forming the cell walls.

The membrane thickness was measured on a scanning electron microscope at 2000–10,000× magnification. All membranes used in the tests had a thickness of 2.8×10^{-3}–5×10^{-3} mm.

The cross-sectional area of the membrane taking part in the permeation process was measured from enlarged photographs. Once the membrane thickness and area are known, the permeability coefficient can be computed from the volumetric flow, partial pressure difference and membrane geometry.

7. FOAM DIFFUSION COEFFICIENT MEASUREMENT

The effective foam diffusion coefficient can be obtained from steady-state permeability measurements. An apparatus similar to those used for the film test was made. During the film tests, thin films are exposed to high partial pressure difference which result in high permeation rates. Foam samples have to be thick, at least 20 cell diameters (10 mm) to eliminate surface effects. Since foam is a compressible material, it should not be exposed to very high pressure. The thick sample and low pressure differential result in a permeation rate which is lower by several orders of magnitude than that for films. The low permeation rate substantially complicates the measurement; any evaporation or outgassing becomes important. To avoid this, only materials having low vapor pressures and diffusion coefficients much lower than the foam D_{eff} can be used in the apparatus.

The apparatus developed for foam permeability measurements is shown in Fig. 3. The cell was made out of stainless-steel and is sealed with indium gaskets. The foam sample, 7.6 cm (3 in) in diameter, up to 2.54 cm (1 in) thick is fixed to a stainless-steel ring by DER

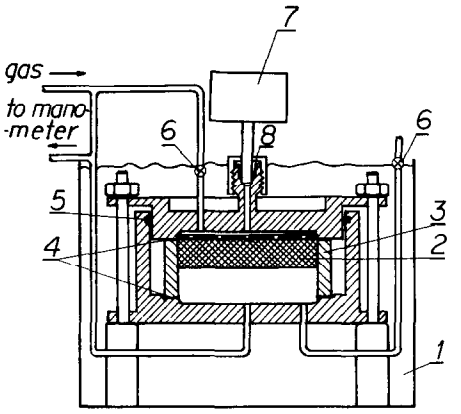

FIG. 3. Apparatus for foam effective permeability measurement. 1, constant temperature bath; 2, foam sample; 3, stainless-steel ring; 4, indium gaskets; 5, O-ring; 6, valves; 7, pressure transducer; 8, indium O-ring.

331 epoxy. The cell was made out of a stainless-steel rod to minimize the welding. All parts of the cell in contact with gas were cleaned ultrasonically.

The permeation rate is found from the pressure increase in the low pressure plenum. The measurement cannot be obtained until steady state conditions are achieved within the foam sample. This requires not only a constant concentration gradient of the test gas but also elimination of other gas components from the sample whose diffusion can lead to erroneous test results. Thus data for CO_2, which rapidly reaches steady state, can not be taken until N_2 is exhausted from the sample— a process which takes about 10 times longer than reaching steady state for the CO_2. Since freon has such a low diffusion rate, it will not contribute significant errors to the test of other gases. The time required to achieve a steady-state partial pressure profile with a particular gas is typically several days to several months. During that time the foam sample must be constantly flushed by a gas on both sides while a pressure difference, 5.5×10^4 Pa (8 p.s.i.), is maintained across the sample.

8. RESULTS AND DISCUSSION

About 20 methane diisocyanate (MDI) and tolylene diisocyanate (TDI) membranes were tested. Only three MDI membranes (Table 1) did not have defects such as microbubbles or pores. Microbubbles were easy to detect under a microscope. The walls of the microbubbles are much thinner than the membrane, so that artificially high permeation rates were measured in membranes having microbubbles.

Membranes having large pores compared to the mean free path of air molecules were easy to detect. Under the pressure difference created by the weight at the slug in the capillary tube, bulk flow much higher than the expected permeation rate was always observed. If the diameter of the pores is smaller than

Table 1. Measured permeability of polyurethane cell walls ($cm^3_{STP}\ cm^{-1}\ s^{-1}\ atm^{-1}$)

Membrane	Density ($kg\ m^{-3}$)	Pe_{CO_2}	Pe_{O_2}	Pe_{N_2}
No. 1, MDI	28.35	16.9×10^{-10}	4.26×10^{-10}	—
No. 2, MDI	25.15	17.5×10^{-10}	4.33×10^{-10}	—
No. 3, MDI	25.15	16.74×10^{-10}	4.46×10^{-10}	0.798×10^{-10}

MDI = methane diisocyanate.

the mean free paths of the air molecules, the so-called Knudsen diffusion occurs [11]. Molecules of N_2, O_2, and CO_2 diffuse with approximately the same rate through these pores, so that the measured permeability coefficient of N_2, O_2 and CO_2 do not have the ratio found for sound films.

The data given in Table 1 indicate that permeability of the cell walls is constant, i.e. that it does not depend on the formation history. Permeability of membranes No. 1 and No. 2 was measured with a capillary tube. Consistent data were not obtained with N_2 since at least 24 h were needed to obtain substantial slug displacement. During that period of time, barometric pressure would usually change, causing additional slug motion and errors in the measured permeability. Membrane No. 3 was tested with an absolute pressure transducer. Therefore data obtained from this membrane are believed to be the most accurate. Membranes No. 1 and No. 3 were obtained from the surface of the foam No. 1.

Figure 4 shows foam data obtained with a pressure transducer for N_2, O_2 and CO_2 at 25°C and 50°C with foam having density $\rho = 25.15\ kg\ m^{-3}$ (sample No. 1). About 120 days were needed to obtain steady-state partial pressure profile with N_2 at 25°C.

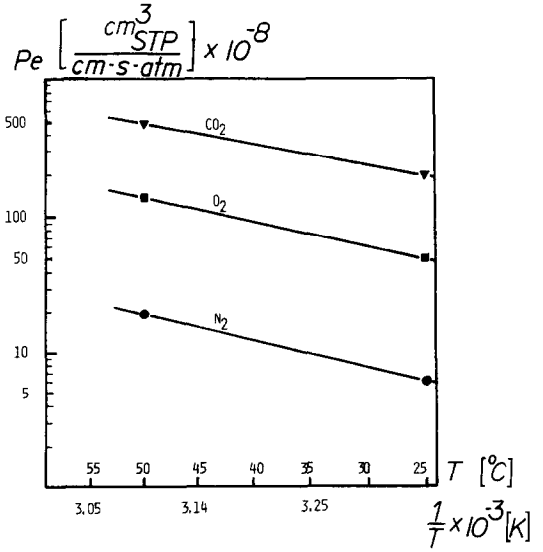

FIG. 4. Permeability of polyurethane foam sample No. 1, to air components (MDI, $\rho = 25.15\ kg\ m^{-3}$).

The foam sample No. 2, having density $\rho = 28.35\ kg\ m^{-3}$ was exposed to various pressure differences of CO_2 at three different temperatures (Fig. 5). The permeability was found to be independent of the pressure difference at each temperature level.

Table 2 presents a comparison of the effective diffusion coefficient predicted by the model, equation (23), and the measured effective diffusion coefficient for foam No. 1, No. 2 and No. 3. Since the effects of the open cells is not included in the model, the model somewhat underpredicts the foam effective diffusion coefficient.

One would expect that permeability of a foam decreases as the foam density increases. However, foam No. 1 has smaller cells and thicker cell walls than foam No. 2 and therefore is less permeable. The model correctly predicts that the less dense foam No. 1 has a lower diffusion coefficient than the more dense foam No. 2.

Foam No. 3 was specially fabricated to have the lowest density, $\rho = 22.5\ kg\ m^{-3}$. At the same time it has the largest average distance between the successive membranes, the thinnest cell walls and a high percentage of open cells. The model correctly predicts that this results in a very low permeation resistance, i.e. a very high diffusion coefficient. The unequal size of the cells was also observed in the SEM photographs of this foam; because of this, the value of the geometric parameters measured on different photographs varied. Consequently, modeled effective diffusion

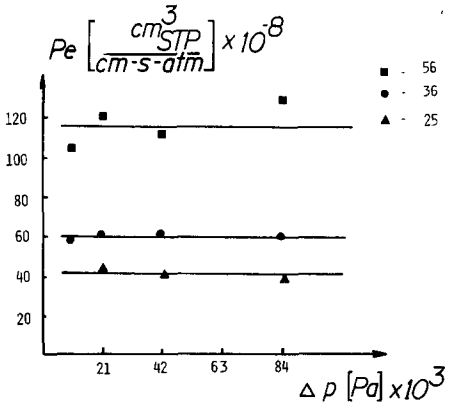

FIG. 5. Permeability as a function of temperature measured at four different pressures. Sample No. 2, $\rho = 28.35\ kg\ m^{-3}$.

Table 2. Comparison between the analytical model and the foam data

Foam	Gas	Successive membrane model, D_{eff}($cm^2\ s^{-1}$)	Foam data, D_{eff}($cm^2\ s^{-1}$)	Error (%)
No. 1, MDI type $\rho = 25.2\ kg\ m^{-3}$ $d = 0.412$ mm $t = 0.60 \times 10^{-3}$ mm $\langle l \rangle = 0.274$ mm $\langle l \rangle / t = 458$	CO_2	15.33×10^{-7}	20.1×10^{-7}	−23.7
	O_2	4.08×10^{-7}	4.68×10^{-7}	−12.8
	N_2	0.73×10^{-7}	0.76×10^{-7}	−3.9
No. 2, MDI type $\rho = 28.35\ kg\ m^{-3}$ $d = 0.51$ mm $t = 0.37 \times 10^{-3}$ mm $\langle l \rangle = 0.34$ mm $\langle l \rangle / t = 919$	CO_2	30.8×10^{-7}	31.7×10^{-7}	−0.3
No. 3, MDI type $\rho = 22.5\ kg\ m^{-3}$ $d = 0.795$–1.08 mm $\langle l \rangle = 0.53$–0.722 $t = 0.28 \times 10^{-3}$ mm $\langle l \rangle / t = 1906$–$2597$ open cells = 26.9%	CO_2	66.5–87.0×10^{-7}	108.3×10^{-7}	−19.7–−38.6

coefficient also varied, as shown in the Table 2. The model underpredicts the foam effective diffusion coefficient by 19.7–38.6% (average 29%) while the percentage of the open cells was found to be 26.9.

9. CONCLUSIONS

The effective diffusion coefficient of a closed-cell foam can be accurately predicted from the analytical model presented. The model could be improved if the effect of the open cells was included.

The measurement of the foam geometry parameters used in the model require 1–2 days, while 6–8 months were needed to obtain the foam data given in Fig. 4. Therefore it is much more efficient to use the cell wall permeability coefficient given in Table 1, measure foam geometry and use the model, than to perform the foam permeability tests.

Acknowledgements—Sponsorship by the U.S. Department of Energy, Energy Conversion and Utilization Technologies (ECUT) Program and the Building Thermal Envelope Systems and Materials Program is gratefully acknowledged. Special thanks are extended to Mr Joseph Carpenter and Mr David McElroy of Oak Ridge National Laboratories for their support of this project. Addition support in the form of materials and expertise on foam formulation was provided by Mr Thomas Allen and Mr David Fair of Mobay Chemical Company.

REFERENCES

1. G. W. Ball, R. Hurd and M. G. Walker, The thermal conductivity of rigid polyurethane foams, *J. cell Plast.* **6**, 66–76 (1970).
2. F. J. Norton, Diffusion of chlorofluorocarbon gases in polymer films and foams, *J. cell. Plast.* **18**, 300–318 (1982).
3. F. J. Norton, Thermal conductivity and life of polymer foams, *J. cell Plast.* **3**, 23–36 (1967).
4. D. A. Brandreth and H. G. Ingersole, Accelerated aging of rigid polyurethane foam, Unpublished report, E.I. du Pont de Nemours and Co., Wilmington, DE.
5. A. G. Ostrogorsky, Aging of polyurethane foams. Sc.D. thesis, Department of Mechanical Engineering, Massachusetts Institute of Technology, Cambridge, MA (1985).
6. E. F. Cuddihy and J. Moacanin, Diffusion of gases in polymeric foams, *J. cell. Plast.* **3**, 73–80 (1967).
7. M. R. Hallinan, W. A. Himmler and M. Kaplan, Advances in the technology of rigid urethane foams, *Eighteenth Annual Technical Conference of the Society of Plastics Engineers*, Section 20–4, p. 2 (1962).
8. D. W. Reitz, A basic study of gas diffusion in foam insulation. S. M. thesis, Department of Mechanical Engineering, Massachusetts Institute of Technology, Cambridge, MA (1983).
9. D. W. Reitz, M. A. Schuetz and L. R. Glicksman, A basic study of aging of foam insulation, *J. cell. Plast.* **20**, 104–113 (1984).
10. D. W. van Krevelrn, *Properties of Polymers*, p. 422. Elsevier, Amsterdam (1976).
11. C. J. Geankopolis, *Mass Transport Phenomena*, p. 151. Holt, Rinehart & Winston, New York (1972).

VIEILLISSEMENT DES MOUSSES DE POLYURETHANE

Résumé—La dégradation des propriétés thermiques des mousses due à la diffusion d'air dans la mousse, appelée vieillissement, est un inconvénient important des mousses polyuréthane. Un modèle analytique est développé pour prévoir le coefficient de diffusion effectif de la mousse et, à partir de lui, le débit de gaz diffusé et le vieillissement de la mousse. Le modèle nécessite une mesure de la perméabilité de la paroi et la connaissance de la géométrie interne de la mousse. Une technique expérimentale de régime permanent est développée pour mesurer la perméabilité des parois de la cellule. Pour tester les modèles une technique expérimentale permet la mesure du coefficient de diffusion effectif. Les prédictions du modèle sont à mieux de 29% les données expérimentales de la mousse.

ALTERUNG VON POLYURETHAN-SCHÄUMEN

Zusammenfassung—Die Degradation der thermischen Eigenschaften von Schaum durch die Diffusion von Luft in den Schaum—bezeichnet als Alterung des Schaumes—ist in erster Linie für den zurückgehenden Einsatz von Polyurethan-Schäumen verantwortlich. Zur Bestimmung des effektiven Diffusionkoeffizienten wurde ein analytisches Modell entwickelt, mit dem die Diffusionsrate des Gases und die Alterung des Schaumes ermittelt wird. Das Modell erfordert die Messung der Permeabilität der Wand und der inneren Geometrie des Schaumes. Eine experimentelle stationäre Methode zur Messung der Permeabilität von Zellwänden wurde entwickelt. Zur Überprüfung des Modells wurde eine experimentelle Methode zur Messung des effektiven Diffusionskoeffizienten von Schaum entwickelt. Die mit dem Modell vorausberechneten effektiven Diffusionskoeffizienten ergeben Daten für den Schaum, die um weniger als 29% von den Meßwerten abweichen.

СТАРЕНИЕ ПОЛИУРЕТАНОВЫХ ПЕНОПЛАСТОВ

Аннотация—Вырождение тепловых свойств пенопласта вследствие диффузии воздуха в него, приводящей к старению, основной недостаток полиуретановых пенопластов. Для расчета эффективного коэффициента диффузии пенопласта развита аналитическая модель, из которой получены скорость диффузии воздуха и старения пенопласта. Для построения модели необходимо знать измеренные значения проницаемости стенки и внутреннюю геометрию пенопласта. Для измерения проницаемости разработан стационарный метод. Для проверки моделей создан экспериментальный метод измерения эффективного коэффициента диффузии пенопласта. Найдено, что рассчитанные на основании модели значения эффективного коэффициента диффузии и экспериментальные данные различаются не более, чем на 29%.